rGO@S Aerogel Cathode for High Performance Lithium-Sulfur Batteries

Ye Chen, Junbo Qin, Junjie You[*]*, Xinyi Chi, Chuanqing Du and Siqing Cheng*

Innovation Centre for Nanomaterials in Energy and Environment (ICNEE), School of Chemical and Environmental Engineering, Wuhan Polytechnic University, Hubei 430023, P. R. China
[*]E-mail: icnee@whpu.edu.cn

A novel approach for the fabrications of rGO@S aerogels wherein the sublimed sulfur was impregnated was proposed based on the reduction of the mixed sol of graphene oxide and sulfur followed by the freeze-dry. The as-obtained rGO@S aerogels as cathode for lithium sulfur battery were investigated electrochemically. The results show that the rGO@S cathode delivers a high discharge specific capacity of more than 1200 mA h g-1 at a current rate of 0.5 C at room temperature and exhibits good cycling stability and excellent rate capability, indicating the faster kinetics and good reversible thermodynamics for the reaction of sulfur in rGO@S aerogels with lithium in lithium sulfur batteries. This might be attributed to the unique porous structure of rGO@S aerogels in which sulfur could be utilized fully.

1. INTRODUCTION

The rapid development for electric vehicles (EVs) urges the lithium ion battery with high specific capacity and good cycle performance.[1, 2] Among the studied lithium ion battery, lithium sulfur battery is the most promising in the foreseeable future to meet the energy requirement of EVs due to its high theoretic specific capacity (1672 mA h g^{-1}) and energy density (2600 W h kg^{-1}), except for low cost, environmental friendliness and easily available resource of sulfur as cathodic material for lithium sulfur battery.[3-5] However, the large-scale commercialization of lithium sulfur battery is impeded in terms of its poor rate capability due to low electrical conductivity of sulfur, low cycling stability thanks to the soluble-easy lithium polysulfide in electrolyte produced during the charge-discharge process to result in the called "shuttle effect", the accessible pulverization of electrode in virtue of the cubical dilatation of ca. 80% during the lithiation and delithiation process of sulfur.[6-9] To overcome these problems, one of the efficacious strategies is to utilize the popular conductive carbon materials such as graphene, carbon

nanotube and porous carbon etc. as sulfur supports to construct sulfur coating composites.[6, 9] Thereinto, graphene aerogel owing to its high conductivity, excellent mechanistical elasticity and high chemical stability has been employed widely in lithium sulfur battery as sulfur support to increase the electroconductivity of cathodic materials, to restrain the shuttle effect and to decrease the loss of the active substance of the electrode.[10-12] In recent years, the three dimensional porous aerogel fabricated by the reduced graphene oxide (rGO) has aroused great interesting as sulfur support for lithium sulfur battery because they could load physically the sublimed sulfur thanks to the constructed porous avenue by graphene sheets with high intensity and are prone to fix chemically the sublimed sulfur as well due to the rich thiophile functional groups containing oxygen, hoisting the utilization of active sulfur. Additionally, it could also be modified on the surface of the porous carbon by some metal oxides to boost the chemical adsorptions of polysulfides which are the intermediate products of sulfur electrode reaction.[13]

The high sulfur load in rGO is an essential prerequisite to guarantee the high capacity of sulfur electrode[14], which infers that it is rather difficult to distribute evenly the sulfur on the porous carbon support. As such, it is of importance to choose suitable method for impregnating sulfur in rGO. Otherwise, it would produce a large amount of "dead sulfur" to decrease the charge and discharge capacity while the poor contact between sulfur and rGO sheet is not beneficial to the effective physical and chemical adsorption of sulfur and the intermediate products by conductive rGO.[15] To the best of our knowledge, two approaches have been developed to fabricate the sulfur/rGO composites for lithium-sulfur batteries: solid melting-permeation combination and solution-deposition combination.[16] The former is to permeate the molten solid sublimed sulfur into graphene or graphene oxide and the latter is to deposit the sublimed sulfur in the solution or by oxidation-reduction reaction of the precursors such as Na_2S_x, $Na_2S_2O_3$ etc. on the graphene or graphene oxide sheets. Wang et al[10] reported the two-step route of "Melting at 200 °C, Evaporation at 300°C" to fabricate sulfur/graphene composites with the high initial discharge specific capacity of 800 mA h g^{-1}. Cui et al[17] prepared sulfur/graphene composite by the in situ sulfur deposition via the oxidation-reduction reaction of $Na_2S_2O_3$ and the obtained composites as the cathode material for lithium sulfur battery delivered a discharge specific capacity of 750 mA h g^{-1} at the current density of 334.4 mA g^{-1}. Similarly, Ji et al[18] obtained the sulfur/graphene nanocomposites by the oxidation-reduction reaction of S_x^{2-} and its discharge specific capacity still remains at 600 mA h g^{-1} at the current density of 830 mA g^{-1} after 140 cycles. Although the sulfur in GO/sulfur composites prepared by the solution-deposition method is distributed evenly, it is environmental unfriendly undoubtedly due to the release of the toxic gas of SO_2 and H_2S during the preparation. Thus, Yang et al[19] proposed one-step preparation of sulfur/graphene nanocomposite by the direct oxidation-reduction reaction with H_2S as a reductant and graphene oxide as an oxidant and the obtained rGO/S nanocomposites exhibited the discharge specific capacity of 950 mA h g^{-1} at the current density of 0.2 A g^{-1}, which has been the paragon of the green synthesis of graphene/sulfur composite for lithium sulfur batteries. However, the most impregnated sulfur of 40 wt% due to the quantitative restriction of the functional group containing oxygen on the surface of graphene oxide is far from satisfying for the practical application of lithium sulfur battery. Therefore, it remains still a challenge to load a high content of sulfur in graphene or graphene oxide using a suitable approach for lithium sulfur batteries.

In this paper, a novel approach for sulfur impregnated in rGO to generate rGO@S aerogel cathode for lithium ion batteries was proposed. The obtained rGO@S aerogel wherein sulfur is distributed evenly could be tuned by the different sulfur content to demonstrate the high capacity lithium sulfur batteries with excellent electrochemical performance.

2. EXPERIMENTAL SECTION

2.2. Materials

All reagents used were purchased from Sinopharm Chemical Reagent Co. Ltd. (Shanghai, China) and used as received without further purification unless otherwise stated.

2.2 Synthesis of graphene oxides

The modified Hummers method[20-22] was employed to prepare the graphene oxide in our experiment. Typically, 150 ml of 98% H_2SO_4 was added slowly into a three-necked flask in which 2 g of natural graphite powder and 1.75 g of $NaNO_3$ were placed while stirring magnetically in an ice water bath for about 5 hours. Then 9 grams of $KMnO_4$ (purity 99%) was added gradually over the course of about 4 hours with stirring slowly. The resultant mixture was subject to reaction for seven days at room temperature. Afterwards, 200 ml of 5 wt% H_2SO_4 aqueous solution was added under slow stirring conditions for about 4 hours followed by adding dropwise 6 ml of 30 wt% H_2O_2 aqueous solution. The mixture was further stirred for 2 hours and then centrifuged to remove the supernatant. The solid phase was continuously washed thoroughly with a mixed aqueous solution of 3 wt% H_2SO_4/0.5 wt % H_2O_2 many times and subjected to disperse in DI water. The brown-black homogeneous graphene oxide dispersion was obtained for the following use.

2.3 Preparation of mixed sol of graphene oxide and sulfur

The sublimed sulfur is insoluble in water and soluble in ethanol so that sulfur sol is generally prepared by the solvent-replaced method. The mixed sol was prepared by adding sulfur alcoholic solution into the above obtained graphene oxide dispersion under ultrasonic condition. Typically, 10 ml of 10 wt% sulfur alcoholic solution was added dropwise into 30 ml of the above prepared brown-black homogeneous graphene oxide dispersion under ultrasonic conditions to obtain the mixed sol.

2.4 Preparation of rGO@S aerogel

40 mg of ascorbic acid was added into the above prepared mixed sol of graphene oxide and sulfur under stirring magnetically. The resultant sol was subjected to reduce in water bath at 95 °C for 3 hours and the container was prefreezed overnight in the freezer compartment after observing the formation of

hydrogel. Then, the sample was continued to heat in water bath at 95 °C to generate the strong hydrogel after the sample was unfreezed. Afterwards, the hydrogel was washed by DI water and freeze-dried to obtain the rGO@S aerogel. Two kinds of rGO@S aerogels with different sulfur content were prepared herein and marked aerogel-A and aerogel-B, respectively. The detailed sulfur content was determined by the following thermogravimetric analysis.

2.5 Material characterization

The weight percentages of sulfur in the rGO@S aerogel were examined by thermogravimetric analysis (TGA) on a Netzsch STA 449 TGA system. A platinum sample pans were used to load the samples and heated to 500 °C from room temperature at the heating rate of 5 °C min^{-1} under a nitrogen atmosphere. The morphology of the rGO@S aerogel was recorded with a high-resolution transmission electron microscopy (HRTEM, JEOL JEM 3010) and the composition of the rGO@S aerogel was analyzed by scanning transmission electron microscope (STEM, F20) equipped with energy dispersive spectrometer (EDS).

2.6 Electrochemical measurements

The aerogel cathode was fabricated by a traditional coating method[23]. Typically, a homogenous slurry consisting of the as-obtained aerogel material (aerogel, 70wt%), and carbon black (CB, 20 wt%), and polyvinylidene fluoride (PVDF, 10 wt%) binder in an N-methyl-2-pyrrolidone (NMP) dispersant was coated uniformly onto an Al foil disks with 10 mm diameter. The typical active sulfur loading was about 1.5 mg /cm^2. A bare sublimed sulfur electrode consisting of 50 wt% sublimed sulfur, 40 wt% of carbon black, and 10 wt% of PVDF binder was prepared in the same way as were the aerogel cathodes. The as-prepared cathodes were dried in a vacuum oven at 80 °C overnight before being transferred into an Argon-filled glovebox (Mikrouna-lab) for the assembly of coin-type cell. The 2032-type coin cells were then assembled in the glovebox by using Li foil as the counter/reference electrode. The used separator is Celgard® 2325 and the used electrolyte is lithium bis(trifluoromethane-sulphonyl)imide (1 mol/dm^3) in 1:1 (v/v) 1, 2 dimethoxyethane and 1, 3-dioxolane (DOL) with LiNO$_3$ (1 wt%) as an additive. The assembled cells were cycled for the measurement of the charged/discharged specific capacity on a programmable battery cycler (LAND, Wuhan, China) from 1.0 to 3.0 V at different current density at room temperature. The redox behavior and the kinetic reversibility of the cell were characterized by the cyclic voltammograms (CV) on a CHI660B electrochemical workstation (Chenghua, Shanghai, China) between 1.0 and 3.0 V. The CHI660B electrochemical workstation was also used to carry out the ac impedance for the as-assembled cells at the open circuit voltage (OCV) with ac amplitude of ± 5 mV and the frequency ranged from 100 kHz to 0.001 Hz.

3. RESULTS AND DISCUSSION
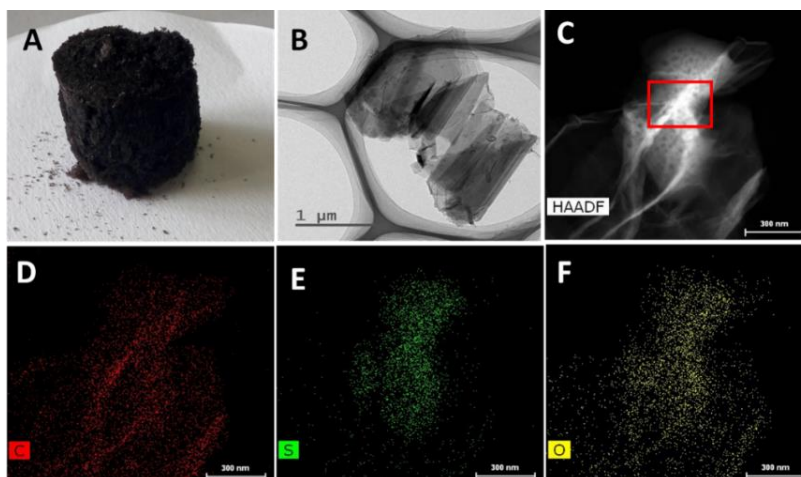
Figure 1. (a) Photograph of an as-prepared aerogel-A; (b) Typical bright field TEM image of an as-prepared aerogel-A at low magnification; (c) Typical STEM image and (d), (e), (f) EDS elemental mapping of the region shown in (c).

Generally, sublimed sulfur is easy to form a sol in water by physical solvent-replaced method, presenting the sulfur nanoparticles evenly distributed in water. Likewise, graphene oxide could also be dispersed well in water under ultrasonic condition to make graphene oxide sol[24-26]. However, the dispersed sublimed sulfur sol is not prone to form sulfur aerogel by aggregation while the graphene oxide sol could be reduced to generate the reduced graphene oxide aerogel. In this work, in order to the evenly distributed sublime sulfur in the reduced graphene oxide aerogel, the mixed sol of graphene oxide and sulfur was prepared and reduced at 95 °C in a water bath using ascorbic acid as a reductant to make an uniform reduced graphene oxide hydrogel containing sulfur sol, followed by the freeze-dried technology to obtain the desired aerogel, as shown typically in Fig.1(a). From Fig.1(a), it is obvious that the obtained rGO@S aerogel tends to be dark grey due to the existence of sublimed sulfur with the density of 0.43 mg/cm^3. To get insight to know the microscopic morphology of the obtained aerogel, the bright field TEM was used to detect the pulverized aerogel. As shown in Fig.1(b) for the typical bright field TEM image of the obtained rGO@S aerogel, it could be seen that the rGO@S aerogel exhibits the lamellar graphene oxide with porous structure in which sulfur is impregnated, which could be further verified by the STEM image in Fig. 1(c). From Fig. 1(c), it looks like the sublimed S nanoparticles were well wrapped with the reduced graphene oxide sheets, indicating the uniformly distributed sublimed sulfur nanoparticles in the obtained aerogel. The elemental composition of the obtained aerogel was confirmed by EDS mapping. Fig. 1d-f present the elemental mapping results for C, O and S in the obtained aerogel, respectively, demonstrating the grown sublimed sulfur nanoparticles inside the graphene oxide. The content of the impregnated sublimed sulfur in the aerogel increases in proportion to the concentration of the sulfur sol in the mixed sol of graphene oxide and sulfur. Thus, two kinds of aerogels with different content of sublimed sulfur (aerogel-A and aerogel-B) were prepared in this paper to compare the electrochemical performance. Their accurate contents of sublimed sulfur were determined using TGA

Int. J. Electrochem. Sci., 17 **(2022)** Article Number: 220251

6

technology. Fig.2 presents the TGA curves of two obtained aerogels. It is indicated that 6.25 wt% and 20 wt% of sulfur were detected and corresponded to aerogel-A and aerogel-B, respectively.
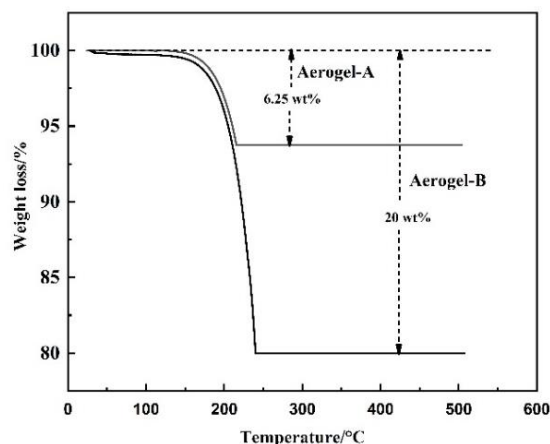

Figure 2. TGA curves recorded in a nitrogen atmosphere with a heating rate of 5°C min^{-1}, for rGO@S aerogel (aerogel-A and aerogel-B).
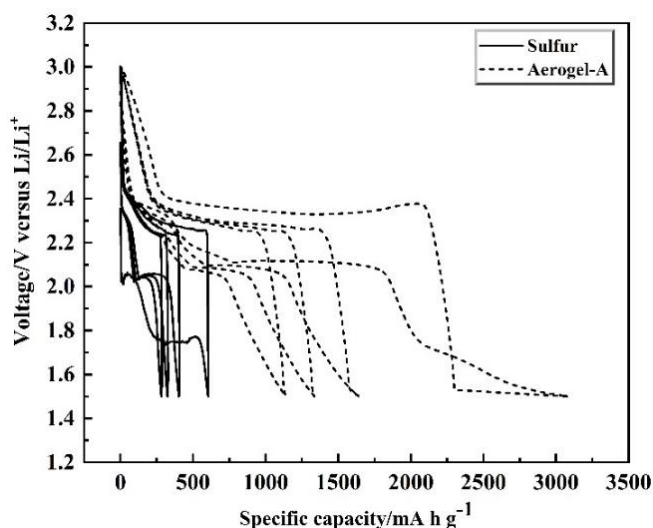
Figure 3. The galvanostatic discharge-charge profiles of the aerogel-A (dashed lines), compared with bare sublimed sulfur itself (solid lines) at a current rate of 0.5 C at various cycles at room temperature.

To evaluate the electrochemical performance of the as-synthesized rGO@S aerogel, 2032-type coin cells were fabricated by rGO@S aerogel as active cathode and lithium foil as the counter electrode. The electrolyte is lithium bis(trifluoromethane-sulfonyl)imide in 1, 2-dimethoxyethane and 1, 3-DOL wherein LiNO$_3$ (1 wt%) is added to passivate the surface of the lithium metal anode and thus ameliorate the severe shuttle effect for lithium sulfur battery. The charge/discharge specific capacities were estimated in terms of the mass of sulfur, as measured by the above thermogravimetric analysis. The

aerogel-A cathode was initially cycled in a voltage window ranged from 1.5 -3.0 V versus Li/Li$^+$ at a constant current rate of 0.5 C (836 mA g^{-1}, 1 C = 1672 mA g^{-1}). To demonstrate and emphasize the synergistic effect of rGO for the electrochemical performance of the as-obtained rGO@S aerogel, the bare sublimed sulfur cathode were also cycled underneath the same measuring conditions for comparison. Fig. 3 presents typical galvanostatic charge-discharge curves for bare sublimed sulfur and aerogel-A electrodes at various cycles at room temperature. From the curved shapes of Fig. 3, it is evident that the discharge curves with two typical plateaus for both the bare sublimed sulfur and aerogel-A should be assigned to the two-step reaction mechanism of sulfur with lithium during the lithiation process while the charge curves with one plateau suggest the vague one-step oxidation of Li$_2$S during the delithiation process[27-29], which would be demonstrated further by the following cyclic voltammograms. Apparently, the performance of low plateau could be improved drastically with aerogel-A cathode compared to the bare sublimed sulfur cathode. However, it is obvious that the uniformly impregnated sublimed sulfur in rGO aerogel shows a serious overcharge effect during the initial discharge and charge process due to the shuttle phenomenon, resulting in the overwhelming initial discharge and charge specific capacities of 3082.4 and 2299.2 mA h g^{-1}, respectively and the low coulombic efficiency of 74.6%. As increasing the cycle number, the discharge specific capacity tends to be stable and decay only 1.5% from 60th to 90th cycle, the coulombic efficiency remains at close 100% after 90 cycles, indicating the successful elimination of shuttle phenomenon due to the rGO framework preventing the loss of sulfur. By contrast, the bare sublimed sulfur cathode only exhibits an initial discharge specific capacity of 603.9 mA h g^{-1} and the discharge specific capacity decay rapidly to be 280 mA h g^{-1} after 90 cycles. All these are compiled in Fig. 4 for the discharge capacities and the coulombic efficiency versus cycle number. It is noticeable that aerogel-B cathode displays an analogous high specific capacity and cycling stability, indicating the remained sulfur utilization with increasing sulfur content, which illustrates the rational preparation of high sulfur loading using the proposed approach in this paper, keeping the active sublimed sulfur dispersed rather than agglomerated during cycling to be dead sulfur. In addition, all these improvement in cyclic durability and high specific capacity of the as-obtained aerogel electrode might be also attributed to the conductive rGO wrapped on the surface of the sublimed sulfur, thus ameliorating the conductivity of the sublimed sulfur electrode. Furthermore, the porous structure of the obtained aerogel might facilitate the full discharge of sulfur owing to the easier electrolyte diffusion into the electrode. More importantly, the strong interaction of the carboxyl group in rGO with those polysulfides during cycling refrains from the dissolution of polysulfides into the liquid electrolyte, alleviating the shuttle effect. Therefore, the conductive rGO as the sublimed sulfur support implement multiple purposes for overcoming the retardation of lithium-sulfur batteries.
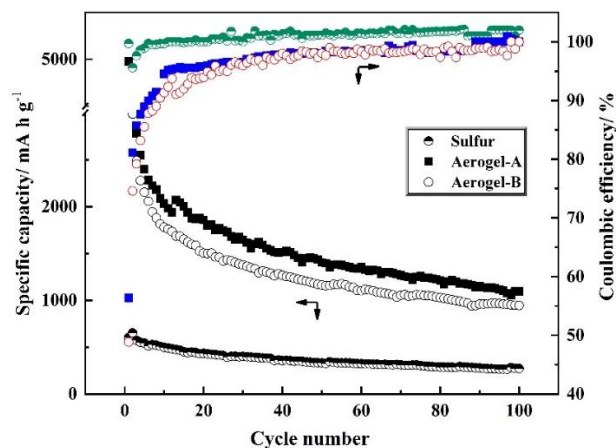
Figure 4. Cycling stability and Coulombic efficiencies of aerogel-A and B cathodes, compared with sulfur cathode itself at a rate of 0.5C. The calculation of specific discharge capacities is based on the mass of sulfur.

To evaluate the rate performance of the rGO@S aerogel cathodes, the aerogel-A cathode was cycled at current rates from 0.5 C to 2 C and then back to 0.5 C, as shown in Fig. 5. it is obvious that the discharge specific capacities for the initial several cycles at the relatively low current rate of 0.5 C decrease with cycling to due to the formation of solid electrolyte interface (SEI) and overcharge effect. As the discharge specific capacity tends to be stable, the aerogel-A exhibits a good cycling stability even though at high current rate of 2 C with the average specific capacity of as high as 995 mA h g^{-1}. The discharge specific capacity for the aerogel-A electrode remained at ca. 1300 mA h g^{-1} when it returns to the current rate of 0.5 C after a rate cycling of 50 cycles. This illustrates the good rate-capability of the rGO@S aerogel cathode, indicating the faster kinetics of the redox reaction of lithium and sulfur in the as-prepared rGO@S aerogel.
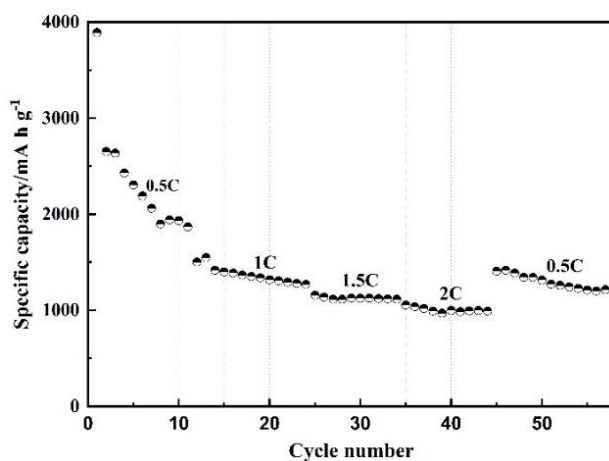
Figure 5. Rate capabilities of aerogel-A cathode cycled at various C-rates from 0.5 C to 2 C

To get further insight to the electrochemical reaction mechanism of the as-obtained rGO@S aerogel cathode for lithium sulfur battery. Cyclic voltammograms (CVs) and electrochemical impedance spectra (EIS) were measured using the bare sublimed sulfur, the as-obtained aerogel-A and B as active cathode materials with metal lithium as anode material, as shown in Fig.6 a and b, respectively. Fig. 6a presents the similar CV results of the electrodes between 1.5 and 3.0 V versus Li/Li$^+$ at a sweep rate of 0.2 mV/s, which is commenced from the open circuit voltage (OCV) about 2.5 V by scanning to lower voltages. From Fig. 6a, two distinguishable reduction peaks are seen obviously, indicating the two-stage reduction mechanism between sulfur and lithium to yield L_2S, as reported previously, which is consistent with the above charge/discharge curves. The first reduction peak takes place at around 2.3 V due to the transformation of sulfur to short lithium polysulfides (Li_2S_n, 2 <n < 8) while the second reduction peak occurs at around 2.0 V owing to the reduction of short lithium polysulfides to lithium sulfide (Li_2S, Li_2S_2).[30-32] The short lithium polysulfides are generally in a metastable state and dissolved easily into the electrolyte, resulting in the shuttle effect and thus capacity degradation during the charge-discharge process. The oxidation peak at around 2.5 V was resulted from the oxidation of Li_2S to short lithium polysulfides and it is not discernible for the oxidation of Li_2S to Li_2S_2 due to the current peak overlap. Furthermore, the as-obtained aerogel-A and B cathodes exhibit rather distinct peak shapes and small potential difference between the oxidation peaks and the reduction peak, suggesting the good reversible thermodynamics for the reaction of sulfur in aerogel-A and B with lithium.
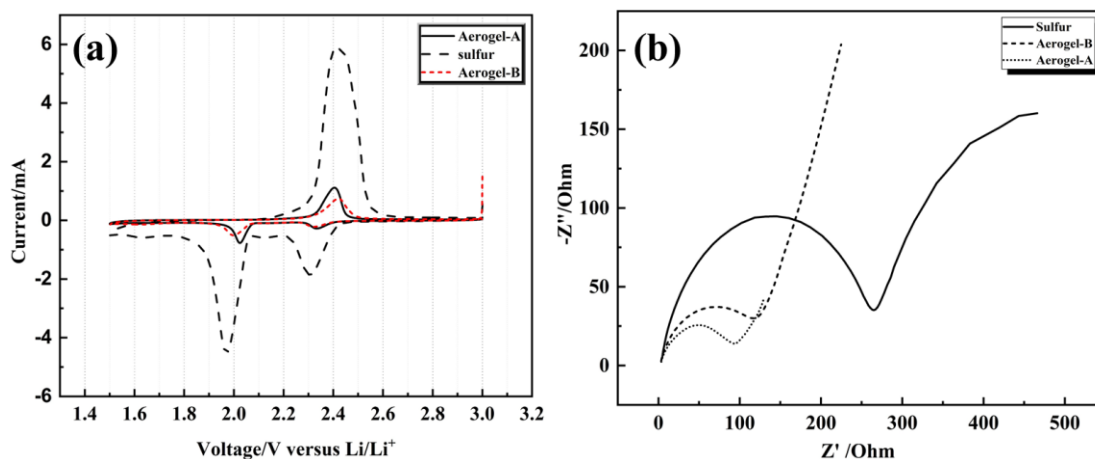
Figure 6. (a) Cyclic voltammograms for bare sublimed sulfur, aerogel-A and B cathodes at a sweep rate of 0.2 mV s^{-1} at room temperature; (b) Nyquist plots of electrochemical impedance spectra of the bare sublimed sulfur, aerogel-A and B cathodes at the OCV of about 2.5 V at the frequency ranged from 100 kHz to 0.001 Hz

Compared with sublimed sulfur, the oxidation peak of aerogel-A cathode seems more negative while that of aerogel-B shifts to be more positive, hinting the polarization difference during lithium ion diffusion due to the formation of insoluble and insulating Li_2S, which could be verified further by the electrochemical AC impedance spectra (EIS) of the investigated cathodes including the bare sulfur, aerogel-A and B. The resulting Nyquist plots are shown in Figure 5b. Obviously, the Nyquist plots of the bare sulfur, aerogel-A and B show the distinct semicircle at high and medium frequency region due to the charge-transfer resistance of Li$^+$ insertion and the straight line with different slope in the low-

frequency region due to the diffusion of Li$^+$ in electrode. Comparing with the diameter of the semicircle, it could be seen that the charge and the Li$^+$ diffusion in the as-obtained rGO@S aerogel cathode transfer faster than those in the bare sublimed sulfur cathode. Furthermore, the charge transfer and the Li+ diffusion in the aerogel-A is faster than that in the aerogel-B, indicating the disadvantageous electrochemical properties with the increasing sulfur content. All of these illuminates further the above obtained electrochemical performance of the as-synthesized rGO@S aerogel.

4. CONCLUSION

rGO@S aerogels wherein the sublimed sulfur is impregnated uniformly are successfully fabricated using the proposed novel method which is to reduce the mixed sol of graphene oxide and sulfur followed by the freeze-dry. The as-prepared rGO@S aerogels as cathode for lithium sulfur battery exhibit high specific capacity of more than 1200 mA h g^{-1} at a current rate of 0.5 C at room temperature and high cycling stability in that the discharge specific capacity decay only 1.5% from 60th to 90th cycle at a current rate of 0.5 C at room temperature with the Coulombic efficiency of up to 100%, suggesting the full utilization of sulfur in rGO@S aerogel and the good reversible thermodynamics for the reaction of sulfur in rGO@S aerogel with lithium. In addition, the excellent rate-capability for rGO@S aerogel cathode is displayed also, indicating the faster kinetics of sulfur in rGO@S aerogel with lithium. These performances of the rGO@S aerogel cathode might be attributed to the unique porous structure of rGO@S aerogel in which the sublimed sulfur is distributed evenly, showing the great potential in EVs as cathode of power battery.

References

1. Y. Q. Chen, Y. Q. Kang, Y. Zhao, L. Wang, J. L. Liu, Y. X. Li, Z. Liang, X. M. He, X. Li, N. Tavajohi and B. H. Li. *J. Energy Chem.*, 59 (2021) 83.
2. F. X. Wu, J. Maier and Y. Yu. *Chem. Soc. Rev.*, 49 (2020) 1569.
3. C. X. Bi, M. Zhao, L. P. Hou, Z. X. Chen, X. Q. Zhang, B. Q. Li, H. Yuan and J. Q. Huang. *Adv. Sci.,* 1 (2021) 2103910.
4. S. Evers and L. F. Nazar. *Acc. Chem. Res.*, 46 (2013) 1135.
5. Z. L. Han, S. P. Li, Y. K. Wu, C. Yu, S. J. Cheng and J. Xie. *J. Mater. Chem.* A, 9 (2021) 24215.
6. A. Eftekhari and D. W. Kim. *J. Mater. Chem.* A, 5 (2017) 17734.
7. Y. Hu, W. Chen, T. Y. Lei, Y. Jiao, J. W. Huang, A. J. Hu, C. H. Gong, C. Y. Yan, X. F. Wang and J. Xiong. *Adv. Energy Mater.*, 10 (2020) 2000082.
8. T. Ould Ely, D. Kamzabek, D. Chakraborty and M. F. Doherty. *Acs. Appl. Energy Mater.*, 1 (2018) 1783.
9. M. Rana, S. A. Ahad, M. Li, B. Luo, L. Z. Wang, I. Gentle and R. Knibbe. *Energy Stor. Mater.*, 18 (2019) 289.

10. H. L. Wang, Y. Yang, Y. Y. Liang, J. T. Robinson, Y. G. Li, A. Jackson, Y. Cui and H. J. Dai. *Nano Lett.*, 11 (2011) 2644.
11. M. Q. Zhao, Q. Zhang, J. Q. Huang, G. L. Tian, J. Q. Nie, H. J. Peng and F. Wei. *Nat. Commun.*, 5 (2014) 5759.
12. G. M. Zhou, L. C. Yin, D. W. Wang, L. Li, S. F. Pei, I. R. Gentle, F. Li and H. M. Cheng. *Acs Nano*, 7 (2013) 5367.
13. J. Q. Huang, Z. Y. Wang, Z. L. Xu, W. G. Chong, X. Y. Qin, X. Y. Wang and J. K. Kim. *Acs Applied Materials & Interfaces*, 8 (2016) 28663.
14. A. Manthiram, Y. Z. Fu and Y. S. Su. *Acc. Chem. Res.*, 46 (2013) 1125.
15. J.-Q. Huang, Q. Zhang and F. Wei. *Energy Stor. Mater.*, 1 (2015) 127.
16. H. F. Li, X. W. Yang, X. M. Wang, M. N. Liu, F. M. Ye, J. Wang, Y. C. Qiu, W. F. Li and Y. G. Zhang. *Nano Energy*, 12 (2015) 468.
17. Y. T. Weng, H. S. Wang, R. C. Lee, C. Y. Huang, S. S. Huang, M. Abdollahifar, L. M. Kuo, B. J. Hwang, C. L. Kuo, Y. Cui and N. L. Wu. *J. Power Sources*, 450 (2020) 227676.
18. L. W. Ji, M. M. Rao, H. M. Zheng, L. Zhang, Y. C. Li, W. H. Duan, J. H. Guo, E. J. Cairns and Y. G. Zhang. *J. Am. Chem. Soc.*, 133 (2011) 18522.
19. C. Zhang, W. Lv, W. G. Zhang, X. Y. Zheng, M. B. Wu, W. Wei, Y. Tao, Z. J. Li and Q. H. Yang. *Adv. Energy Mater.*, 4 (2014) 1301565.
20. D. R. Dreyer, S. Park, C. W. Bielawski and R. S. Ruoff. *Chem. Soc. Rev.*, 39 (2010) 228.
21. D. C. Marcano, D. V. Kosynkin, J. M. Berlin, A. Sinitskii, Z. Z. Sun, A. Slesarev, L. B. Alemany, W. Lu and J. M. Tour. *Acs Nano*, 4 (2010) 4806.
22. Y. W. Zhu, S. Murali, W. W. Cai, X. S. Li, J. W. Suk, J. R. Potts and R. S. Ruoff. *Adv. Mater.*, 22 (2010) 3906.
23. W. Zhou, Y. R. Wang, L. P. Zhang, G. S. Song and S. Q. Cheng. *Int. J. Electrochem. Sci.*, 10 (2015) 5061.
24. Z. L. Wang, D. Xu, J. J. Xu, L. L. Zhang and X. B. Zhang. *Adv. Funct. Mater.*, 22 (2012) 3699.
25. M. A. Worsley, P. J. Pauzauskie, T. Y. Olson, J. Biener, J. H. Satcher and T. F. Baumann. *J. Am. Chem. Soc.*, 132 (2010) 14067.
26. S. Z. Zu and B. H. Han. *J. Phys. Chem.* C, 113 (2009) 13651.
27. D. Aurbach, E. Pollak, R. Elazari, G. Salitra, C. S. Kelley and J. Affinito. *J. Electrochem. Soc.*, 156 (2009) A694.
28. J. C. Guo, Y. H. Xu and C. S. Wang. *Nano Lett.*, 11 (2011) 4288.
29. X. Liang, C. Hart, Q. Pang, A. Garsuch, T. Weiss and L. F. Nazar. *Nat. Commun.*, 6 (2015) 6682.
30. N. S. Choi, Z. H. Chen, S. A. Freunberger, X. L. Ji, Y. K. Sun, K. Amine, G. Yushin, L. F. Nazar, J. Cho and P. G. Bruce. *Angew. Chem. Int. Ed.*, 51 (2012) 9994.
31. X. L. Ji, K. T. Lee and L. F. Nazar. *Nat. Mater.*, 8 (2009) 500.
32. X. L. Ji and L. F. Nazar. *J. Mater. Chem.*, 20 (2010) 9821